Primljen / Received: 11.4.2023.
Ispravljen / Corrected: 19.6.2023.
Prihvaćen / Accepted: 4.8.2023.
Dostupno online / Available online: 10.11.2023.

Controlled shaped-charge blasting technology for deep underground tunnel engineering

Authors:

[1]Junlin Lv, PhD. CE
JLLv_sdtbu@163.com
Corresponding author

[1]Binbin Zheng, PhD. CE
348392802@qq.com

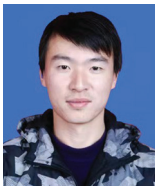

[1]Zhen Liu, PhD. CE
201913693@sdtbu.edu.cn

[2]Junhong Huang, PhD. CE
junhonghuang@whut.edu.cn

[1] Shandong Technology and Business University, China
Faculty of Management Science and Engineering
[2] Wuhan University of Technology, China
Faculty of Resources and Environmental Engineering

Research Paper

Junlin Lv, Binbin Zheng, Zhen Liu, Junhong Huang

Controlled shaped-charge blasting technology for deep underground tunnel engineering

With the rapid development of the economy and society, the demand for mineral resources and energy has increased rapidly. However, it is difficult to improve the efficiency of blasting construction and control the stability of the surrounding rock in deep underground engineering. In this study, the deep underground tunnel of the Tianchi pumped-storage hydropower station in China was considered as the engineering background. Based on the stress redistribution state of the surrounding rock after blasting excavation, the crack propagation effect and dynamic response of the surrounding rock under different controlled blasting methods were studied through theoretical analyses, numerical simulations and in situ tests. The mechanism of directional crack formation was analysed by considering the influence of hole spacing and in situ stress. It was shown that the initial ground stress was conducive to the propagation of the blasting crack in the contour hole of smooth blasting towards the direction line of the blast hole. The test results showed that using controlled shaped-charge blasting methods in the blasting excavation of underground tunnels can improve the utilisation rate of explosives, reduce blasting vibration and achieve a significant effect on directional crack formation. The research results have important engineering significance as they can lead to improvements in the blasting technique, a contour-forming effect of the blasting excavation and control of the stability of the surrounding rock.

Key words:
tunnel engineering, controlled fracture blasting, directional fracture, surrounding rock damage, crack propagation

Prethodno priopćenje

Junlin Lv, Binbin Zheng, Zhen Liu, Junhong Huang

Tehnologija kontroliranog miniranja kumulativnim nabojem za izradu dubokih podzemnih tunela

S brzim razvojem gospodarstva i društva značajno je porasla potražnja za mineralnim sirovinama i energijom. Međutim, teško je poboljšati učinkovitost miniranja i kontrolirati stabilnost okolnih stijena tijekom izrade konstrukcija u dubokom podzemlju. U ovom je radu kao tehnička osnova upotrijebljen duboki podzemni tunel reverzibilne hidroelektrane Tianchi u Kini. Na temelju stanja preraspodjele naprezanja okolnih stijena nakon iskopa miniranjem, teorijskim analizama, numeričkim simulacijama i in situ ispitivanjima istraženi su učinci širenja pukotina i dinamički odziv okolne stijene na temelju različitih metoda miniranja. Provedena je analiza mehanizma usmjerenoga stvaranja pukotina s obzirom na utjecaj razmaka bušotina i in situ naprezanja. Pokazalo se da početno naprezanje tla potiče širenje pukotina pri miniranju u konturnoj bušotini nastaloj glatkim miniranjem u smjeru pravca minske bušotine. Rezultati testiranja pokazali su da je primjenom kontroliranih metoda miniranja kumulativnim nabojem podzemnih tunela moguće povećati stopu iskorištenosti eksploziva, smanjiti vibracije pri miniranju i postići značajan učinak na usmjereno formiranje pukotina. Rezultati istraživanja od velike su važnosti za građevinarstvo jer mogu dovesti do poboljšanja tehnologije miniranja, učinka stvaranja kontura miniranjem i kontrole stabilnosti okolne stijene.

Ključne riječi:
izgradnja tunela, kontrolirano miniranje, usmjereni lom, oštećenje okolne stijene, širenje pukotine

1. Introduction

With the vigorous development of national infrastructure, an increasing number of large-scale projects are advancing into deep underground spaces. They primarily involve hydropower, mining, national defence, and other deep underground engineering projects. The drilling and blasting method is a traditional process used in the excavation of underground chambers and has the advantages of high efficiency and flexibility to adapt to various special geological conditions. However, it also produces many negative effects, such as blasting flying rock, over and underbreak, blasting vibration, and great damage to the rock mass under the condition of high ground stress and other adverse effects [1]. Controlled shaped-charge blasting technology offers significant technical and economic advantages for directional fracture blasting. The controlled shaped-charge blasting technology has a significant effect on increasing the distance between blast holes, reducing the number of holes drilled, improving the utilisation rate of explosive energy, and reducing the damage of blasting excavation to the surrounding rocks. Moreover, this technology is also useful to improve adverse geological conditions (high ground stress, jointed rock mass, weak interlayer, etc.) in deep underground blasting excavation.

Pugh [2] proposed a quasi-steady theory of jet flow that laid the theoretical foundation for studying the formation of shaped-charge jets. Hirsch [3] studied shaped-charge jets using a theoretical analysis and provided a computational model for the angle distribution deviating from the symmetry axis of the shaped-charge jets. Hayes [4] conducted extensive research on the explosive forming effect of a medicine-type cover structure of shaped-charge blasting in tuff. He [5] proposed a new method for bidirectional shaped-charge tensile blasting and introduced the mechanism of shaped-charge blasting in detail from the perspective of the mechanical behaviour of blasting according to the characteristics of the shaped-charge device. A blasting test was conducted at the engineering site, and a good blasting effect was obtained, which proved that the shaped-charge blasting technology has broad application prospects in blasting excavation. Fu [6] used the DYNA3D software to perform a numerical simulation analysis of the formation process of a shaped-charge jet. By comparing the characteristics of the ring- and linear-shaped charges with the same profile structure, the distribution characteristics of the ring-shaped charge jet parameters were analysed. Duan [7] used numerical simulations and experimental research methods based on linear cumulative cutting theory to analyse jet formation, target penetration, and the entire cutting process in shaped-charge blasting, and optimised the parameters of the cutting tool. Satisfactory cutting results were obtained from the experiments. Xu [8] studied the penetration effect of different materials and shapes of medicine-type covers with shaped charges by combining experiments and numerical simulations. Wang [9] used the three-dimensional dynamics software ANSYS/LS-DYNA to perform a numerical analysis of a bipolar charge jet and concluded that the jet formed successfully, penetrated the concrete target, and caused damage. A PVC pipe was used as the shaped pipe material, and the directional fracture-forming technology of rock presplitting blasting was successfully developed through field tests.

Therefore, to form directional cracks between blast holes and improve the forming quality of the contour surface after blasting excavation, the study of fine blasting technology, such as controlled shaped-charge blasting, is of great significance for the development of underground controlled blasting technology and provides theoretical guidance for the construction technology and parameter optimisation in underground blasting excavation. It has important research value for the formation of contour surfaces and the improvement of construction safety in deep-ground engineering.

2. Mechanism of crack propagation in rock mass induced by controlled shaped-charge blasting

2.1. Theoretical research on shaped-charge jets

According to the basic theory of instantaneous detonation, the detonation product moves in the direction normal to the external surface of the material after detonation. Therefore, after the PVC shaped-charge tube was attached to the external surface of the explosive, the detonation wave was transferred along the normal direction of the plane of the shaped-charge groove after detonation and eventually converged in the axis direction of the shaped-charge groove, forming a high-density, high-speed, and high-pressure gas jet. When the jet formed after the explosive initiation acts on the rock to initiate cracks in the blast holes, the explosive gas quickly enters the cracks to produce a "gas wedge" effect on the rock, which further expands the cracks and thus forms directional cracks in the rock [10].

The velocity of the explosive detonation depends on the velocity of the detonation wave, detonation product, and expansion velocity of the gas mixture. The theoretical value of the airflow velocity at the centre of the jet flow is as follows [11]:

$$v_k = \frac{1+\frac{U}{C}\sin\alpha+\left(\frac{U}{C}\right)^2+\sqrt{1+2\frac{U}{C}\sin\alpha+\left(\frac{U}{C}\right)^2\cos\alpha}}{\sin\alpha+\frac{U}{C}} \quad (1)$$

In Eq. (1), α is the angle between the bus bar and the axis of the shaped-charge medicine-type cover. C represents the sonic speed after the detonation wave peak, and C = 3/4D, where D is the speed of the explosive detonation. U is the velocity of the detonation product after the detonation wave, and U = 1/4D.

According to the research results of Li [12], the effective portion of the charge was analysed separately in the direction of the shaped charge. As shown in Figure 1, the detonation products flying away after detonation generated two air streams on the surface of the shaped-charge groove, whose pressures were P_1 and P_2, and the two air streams collided on the angle bisector of the shaped-charge groove. Assuming that the collision is an ideal elastic collision, the detonation pressure after superposition can

be obtained according to the principle of vector superposition, as shown in Figure 2.

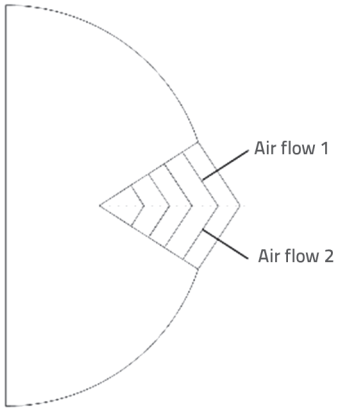

Figure. 1. Diagram of effective

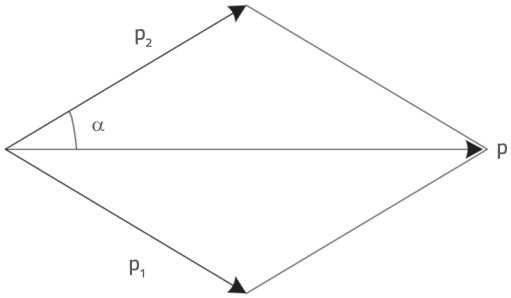

Figure 2. Diagram of pressure partial scattering calculation

$$p_1 = p_2 = \frac{2u^2\rho_0 W}{W+u} \tag{2}$$

In Eq. (2), u is the scattering velocity, Wis the velocity of scattering surface displacement, and ρ_0 is the explosive density. The pressure formed by superposition of p_1 and p_2 is

$$p = \frac{\sin(\pi - 2\alpha)}{\sin\alpha} \tag{3}$$

Substituting Eq. (2) into (3), we obtain

$$p = \frac{2u^2\rho_0 \sin(\pi - 2\alpha)}{(W+u)\sin\alpha} \tag{4}$$

When the two air streams collided and converged, they rapidly spread. Considering that the charging form is linear and the uncoupling coefficient is relatively large, the secondary flow under the assumption of instantaneous detonation can be approximately satisfied, and the airflow pressure is as follows:

$$p_b = p\left(\frac{R_0}{r}\right)^{\nu-1} \tag{5}$$

where R_0 is the radius of the explosive, r is the distance from the centre of the explosive and ν is the power exponent of a one-dimensional flow.

Substituting p in Eq. (4) into (5) and ν = 2, we obtain:

$$p_b = \frac{2u^2\rho_0 W R_0 \sin(\pi - 2\alpha)}{(W+u)r\sin\alpha} \tag{6}$$

When the detonation product collides with the hole wall, the pressure on the hole wall is amplified, and the peak value of the pressure on the hole wall in the direction of energy accumulation is:

$$p_b = \frac{2u^2\rho_0 W R_0 \sin(\pi - 2\alpha)}{(W+u)r_0\sin\alpha} n \tag{7}$$

In Eq. (7), *n* is the amplification factor and r_0 is the radius of the hole.

2.2. Mechanism of explosive crack growth

According to the fracture mechanics theory, under quasi-static pressure, the initiation and propagation of the initial crack should satisfy the following conditions:

$$K_I > K_{IC} \tag{8}$$

$$K_I = pF\sqrt{\pi(r_0 + l_c)} \tag{9}$$

In Eq.s (8) and (9), K_I is the stress intensity factor at the crack tip; K_{IC} is the dynamic fracture toughness of the rock; p is the pressure on the hole wall; F is the correction factor of the stress intensity factor, which is a function of r_0 and l_c, satisfying the relation of Eq. (10) [13]; r_0 is the radius of the blast hole; and l_c is the length of crack growth.

$$p < \frac{K_{IC}}{F\sqrt{\pi(r_0 + l_c)}} \tag{10}$$

3. Numerical simulation analysis of controlled shaped-charge blasting

3.1. Numerical calculation method

The law and distribution of crack growth were studied under different controlled blasting methods. The fluid–solid coupled model was used for the numerical simulation of blasting excavation of rock mass and according to the computational characteristics of the dynamic finite element LS-DYNA software, the Euler algorithm was used for fluid materials such as explosives and air and the Lagrange algorithm was used for solid materials such as rocks. The interactions between the different fluids and solid materials were then investigated. During the calculation, the detonation product and fluid material flowed in the Euler grid without causing grid distortion. In this algorithm, the fluid and solid matter interact with each other through fluid–solid coupling, and the entire process of action of

Table 1. Parameters of the rock emulsion explosive and JWL balance equation, parameters of the emulsion explosive and JWL constants

ρ [g/cm³]	*D* [m/s]	*A* [GPa]	*B* [GPa]	R_1	R_2	ω	*E* [J/m]
1.0	3200	214	0.18	4.15	0.95	0.13	4×10^9
ρ - explosive density; D - detonation velocity							

Table 2. Air material parameters

ρ_2 [g/cm³]	C_p	S_1	S_2	S_3	0	E_2 [J/m³]
1.02	0.1647	2.56	1.986	1.2268	0.5	1.0

Table 3. Material parameters of the shaped-charge tube

Density [g/cm³]	Specific heat [J·K⁻¹·kg⁻¹]	Poisson's ratio	Melting temperature [°C]	Modulus of elasticity [GPa]
1.3	1.18	0.38	95	31

Table 4. Physical and mechanical properties of rocks

Density [g/cm³]	Modulus of elasticity [GPa]	Poisson's ratio	Compressive strength [MPa]	Tensile strength [MPa]
2.7	45	0.23	143	16

the explosive on the rock mass after detonation is described, which can simulate the rock blasting process more accurately [14, 15]. Therefore, the multimaterial fluid–solid coupling algorithm in the LS-DYNA dynamic finite element program was used for the simulation calculation. When a numerical simulation of blasting excavation is performed, the relevant materials and state control equations are as follows.

The high-energy explosive material *MAT_HIGH_EXPLO-SIVE_BURN, combined with the JWL equation of state, was used to simulate the relationship between pressure and volume during explosions. The Eq. is as follows [16]:

$$P = A\left(1-\frac{\omega}{R_1V}\right)e^{-R_1V} + B\left(1-\frac{\omega}{R_2V}\right)e^{-R_2V} + \frac{\omega E_0}{V} \quad (11)$$

In Eq. (12), V is the change in volume, A, B, ω, R_1, R_2 and E_0 represent the material constants, and the specific value is determined according to the type of explosive selected. The specific parameters are listed in Table 1.

The LS-DYNA constitutive model *MAT_NULL was selected as the constitutive model of the air medium, and the *EOS_GRUNEISEN equation of state was defined [17].

$$P = \frac{\rho_2 C_0^2 \mu_0\left[1+\left(1-\frac{\gamma_0}{2}\right)\mu_0 - \frac{\mu_0^2}{2}\right]}{\left[1-(S_1-1)\mu_0 - S_2\frac{\mu_0^2}{\mu_0+1} - S_3\frac{\mu_0^2}{(\mu_0+1)^2}\right]} + (\gamma_0+\alpha_0\mu_0)E_2 \quad (12)$$

In Eq. (13), ρ_2 is the density of the air material; γ_0 is the Gruneisen parameter; C_0 is the curve intercept; α_0 is the first-order volume correction of γ_0; S_1, S_2 and S_3 are the slope coefficients of the curve; and μ_0 is the revised quantity of volume. The parameter values are listed in Table 2.

Polyvinyl chloride (PVC) is currently one of the most widely used plastic materials and has been selected as the material for energy-gathering pipes. Its physical properties are as follows. PVC begins softening at 65–85 °C, attains a fluid state at 170 °C, decomposes with the increase in temperature, and releases a large amount of gas when it reaches 190 °C [18, 19]. The J-C material model is typically used to simulate a shaped-charge cap. The following equation characterises the effective yield stress in the J-C model.

$$\sigma_y = \left(A + B\bar{\varepsilon}^{p^n}\right)\left(1+C\ln\dot{\varepsilon}^*\right)\left(1-T^{*m}\right) \quad (13)$$

In Eq. (14), σ_y is the effective yield stress, $\bar{\varepsilon}^p$ is the equivalent plastic strain, $\dot{\varepsilon}^*$ is the normal effective plastic strain rate, T* is the relative temperature, A is the yield stress, B is the strain hardening coefficient, n is the strain hardening index, C is the strain rate correlation coefficient; and m is the temperature correlation coefficient. $(A+B\varepsilon^{pn})$ represents the function of stress and strain, whereas $\varepsilon^* = 1{,}0$ and $T^* = 0$. $(1+C\ln\varepsilon^*)$ i $(1-T^*_m)$ represent the influences of strain rate and temperature, respectively.

The *MAT_PLASTIC_KINEMATIC material model was used for the rocks. To directly reflect the crack generation and propagation in the blasting process, the keyword *MAT_ADD_EROSION was added. During the calculation process, the program automatically removed the stress units that satisfied the failure criterion, which clearly showed the crack distribution.

3.2. Numerical calculation results of detonation crack propagation under different hole spacing

The directional crack formation mechanism of controlled shaped-charge blasting and the crack propagation between

blast holes were studied. An ANSYS/LS-DYNA dynamic finite element was used to simulate the crack formation process of the underground rock mass in controlled conventional blasting and controlled shaped-charge blasting. To facilitate a comparative analysis, two controlled blasting methods were set up under the same conditions for the numerical calculation. According to the analysis results of Zhou [20], in the controlled shaped-charge blasting model, the thickness of the shaped-charge tube was 2 mm, the angle of the shaped-charge groove was 80°, and the depth of the shaped-charge groove was 5.6 mm. A model of the shaped-charge tube is shown in Figure 3.

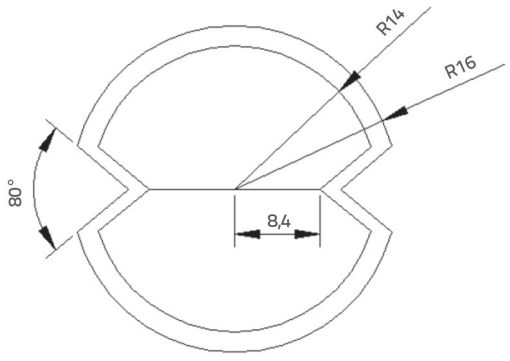

Figure 3. Model size of the shaped-charge tube (unit: mm)

A two-dimensional computational model was established, in which Z-direction constraints were applied to the front and back interfaces of the model, symmetric constraints were applied to the left and right boundaries of the model, and nonreflecting boundary conditions were applied to the upper boundary. The smooth blasting method was adopted for the excavation of the underground tunnel of the Tianchi-pumped storage power station. Therefore, a free boundary was set at the lower boundary of the model to simulate the excavation of the blasting layer. In the calculation model, the diameter of the blast hole was 42 mm, the diameter of the explosive was 32 mm, and the distance between the blast holes was X.

3.2.1. Crack propagation effect of controlled conventional blasting under different hole spacings

Conventional blasting was performed using contour holes. The designed diameter of the blast holes was 42 mm, and the type of explosive used was No. 2 rock emulsion explosive, which was manufactured into an explosive cartridge with a diameter of 32 mm, length of 220 mm, and weight of 200 g. The properties of the borehole charge were as follows: the depth of the cutting holes was 3.4 m, the depth of the auxiliary holes was 3 m, the depth of the contour holes was 3.1 m, the spacing of the contour holes was 0.5 m, the thickness of the blasting layer was 0.5 m, the row spacing of the contour holes was 0.5–0.8 m, the thickness of the blasting holes was 0.6–0.9 m, and the hole spacing of the contour holes was 0.5 m. The specific drilling and blasting parameters are listed in Table 5.

To study the law of crack propagation in controlled conventional blasting, five hole spacings were set for the calculation, as shown in Figure 4. As can be observed from the crack propagation effects of the five different blasting conditions, the number of cracks generated between the holes and the degree of damage to the surrounding rock have significant differences with the change in spacing between the two holes. In addition, after the two holes were simultaneously detonated, a main crack of a certain length was generated in the straight direction of the hole. Simultaneously, because the energy of the explosive was transferred in all directions of the hole wall after detonation, the rock mass was randomly damaged from the hole wall to the inside, forming cracks and causing serious damage to the surrounding rock. The maximum depth of damage to the surrounding rock caused by controlled conventional blasting was 40 cm. The existence of free surfaces has a good guiding effect on the propagation of detonation cracks; therefore, the number and length of cracks on the side near the free surface are significantly increased compared with those on the side of the reserved rock mass.

After explosive initiation, the explosive energy was transferred to the rock mass from the blast hole, causing damage to the rock.

Table 5. Design parameters of conventional blasting

Hole designation	Number of holes (A)	Hole depth [m]	Hole charge		Number of detonator segments (section)
			Mass per hole [kg/hole]	Total mass [kg]	
Cut slot	4	3.4	2.2	8.8	Ms1
Auxiliary hole	8	3	2	16	Ms3
Auxiliary hole	12	3	2	24	Ms5
Auxiliary hole	26	3	2	52	Ms7
Auxiliary hole	16	3	2	32	Ms9
Bottom hole	9	3	2	18	Ms11
Contour pore	32	3.1	0.6	19.2	Ms13
Total	107	/	/	172	/

The explosive energy gradually dissipated and attenuated during transmission. When the energy was attenuated to the extent that the rock was not damaged, the length of the blasting crack ceased to increase. Therefore, as the spacing between the two holes increased, the number and length of blasting cracks decreased. By observing the main cracks under different hole spacings in Figure 4, it can be observed that the main cracks formed between the two blast holes in controlled conventional blasting cannot be well connected along the connection direction of the blast hole. Only with spacings between the blast holes of 50 and 60 cm, the main cracks generated between the two blast holes became roughly connected along the connection direction of the blast hole, as shown in Figure 4.a and 4.b, realising the purpose of excavation of the blasting layer. However, because of the transfer of explosive energy around the hole, it could not concentrate on the connection direction of the hole, resulting in significant damage to the reserved rock mass, which is not conducive to the formation of a stable underground space structure after excavation. When the hole spacings were 70 and 80 cm, as shown in Figure 4.c and 4.d, after explosive initiation, when the generated main crack extended to a certain length in the connection direction of the blast hole, the gradual decay of explosive energy led to deflection of the crack; thus, it deviated from the connection direction of the blast hole and slowly expanded to both sides until the crack tip intersected with the main crack. The reason is crack propagation in which a prominent overbreak and under-excavation phenomenon occurs in actual engineering excavation, and satisfactory excavation effects cannot be achieved. When the spacing between the holes was 90 cm, as shown in Figure 4.e, the main blasting crack between the two holes did not penetrate because of the excessively large spacing between the holes.

In summary, during the excavation of controlled conventional blasting, when the spacing between the two holes was less than 60 cm, the main cracks generated penetrated in a direction that was roughly parallel to the straight line of the blast holes. However, long cracks were generated in other directions of the hole, and numerous secondary cracks were generated on both sides of the main cracks, causing excessive damage to the surrounding rock. Therefore, the crack-control effect of conventional blasting is unsatisfactory.

To reflect the entire process of initiation, propagation, and penetration of controlled conventional blasting cracks more intuitively, a calculation model with a spacing of 60 cm between holes was considered as an example to analyse the propagation process of explosion-induced cracks between two holes after detonation. As shown in Figure 5, after the two holes were detonated, the rock around the hole wall was damaged by the explosion, producing initial cracks. Subsequently, the explosion stress and gas promoted crack propagation. At 100 μs, a certain length of the main crack was formed in the direction of the connecting line between the two blast holes. During the propagation of the main crack, it tended to deviate from the direction of the blast hole line, and secondary cracks formed on both sides of the main crack. Subsequently, the crack continued to expand under the combined action of the

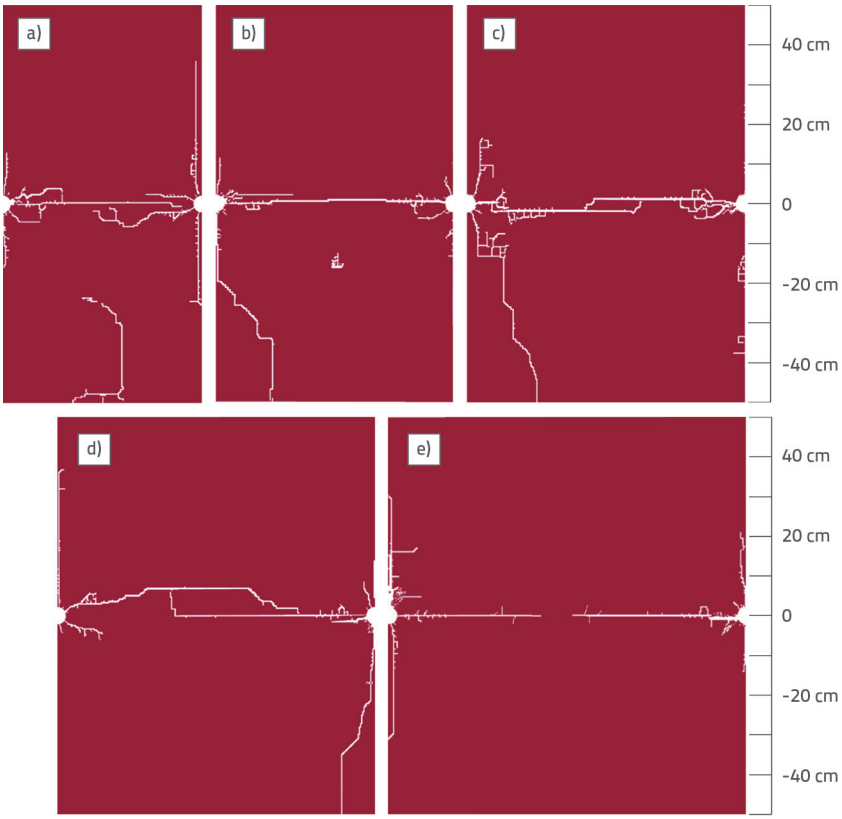

Figure. 4. Conventional blasting effects under different hole spacings: a) 50 cm; b) 60 cm; c) 70 cm; d) 80 cm; e) 90 cm

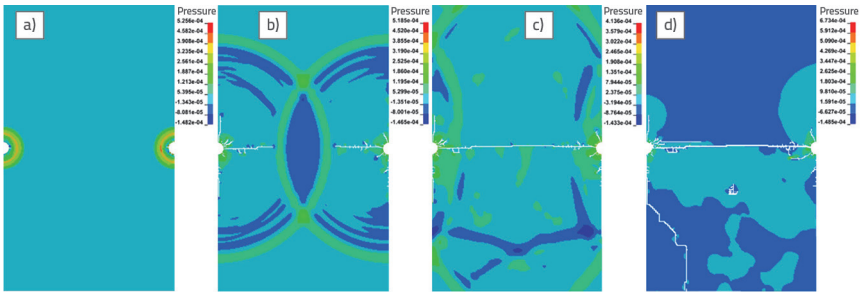

Figure 5. Controlled conventional blasting crack penetration process: a) t = 10 μs; b) t = 100 μs; c) t = 220 μs; d) t = 600 μs

detonation gas, explosion stress, and reflected tension waves formed through the free surface. At 220 μs after detonation, the main crack of the two blast holes was connected in a direction roughly parallel to the line of the blast holes, whereas the crack further expanded in other directions around the blast holes. After the main crack was connected, the explosive gas continued to expand within the crack, promoting an increase in the crack width. Under the action of the reflected tensile waves, the crack extended to the free surface. With the dissipation and attenuation of energy, the cracks stop expanding in the rock.

3.2.2. Crack propagation effect of controlled shaped-charge blasting under different hole spacings

To study the law of crack propagation in controlled shaped-charge blasting, five hole spacings were set for calculation and analysis, as shown in Figure 6. It can be observed from the crack distribution under these five different hole spacing conditions that the number of cracks produced by controlled shaped-charge blasting, the distribution form, and the degree of damage to the surrounding rock have obvious differences. As shown in Figure 6.a to 6.d, with spacing of 50 to 80 cm between the two holes, the main cracks were generated in the straight connection line between the blast holes after simultaneous detonation. This has an ideal effect on the formation of directional cracks, achieving the purpose of blasting excavation and reducing the degree of damage to the surrounding rock. Moreover, the phenomena of over-excavation and under-excavation did not occur. Owing to the guiding effect of the shaped-charge groove, more explosive energy acts on the rock in the straight direction between the blast holes. This promotes the formation of the main cracks, thus reducing the energy acting on the rock in the non-connected direction between the blast holes. Thus, only a small number of short cracks are generated in the non-connected direction. The damage range of the controlled shaped-charge blasting to the surrounding rock was within 15 cm under the five different hole spacings, and the degree of damage to the surrounding rock was relatively low. The number and length of cracks on the side near the free surface are clearly increased compared to those on the side of the reserved rock mass because the blast stress wave forms reflected tensile waves on the free surface. With spacing between the blast holes of 50–70 cm, as shown in Figure 6.a to 6.c, many secondary cracks were formed on both sides of the main crack during the development and expansion of the main crack, and these secondary cracks were randomly distributed. This indicates that the rock was preferentially destroyed, cracked, and developed to form the main crack in the direction of energy accumulation on the wall of the blast hole after explosive initiation. At the same time, during the propagation process of the main crack, the explosive gas continuously wedged into the main crack, and the comprehensive action of the blast stress wave led to the initiation of secondary cracks on both sides of the main crack.

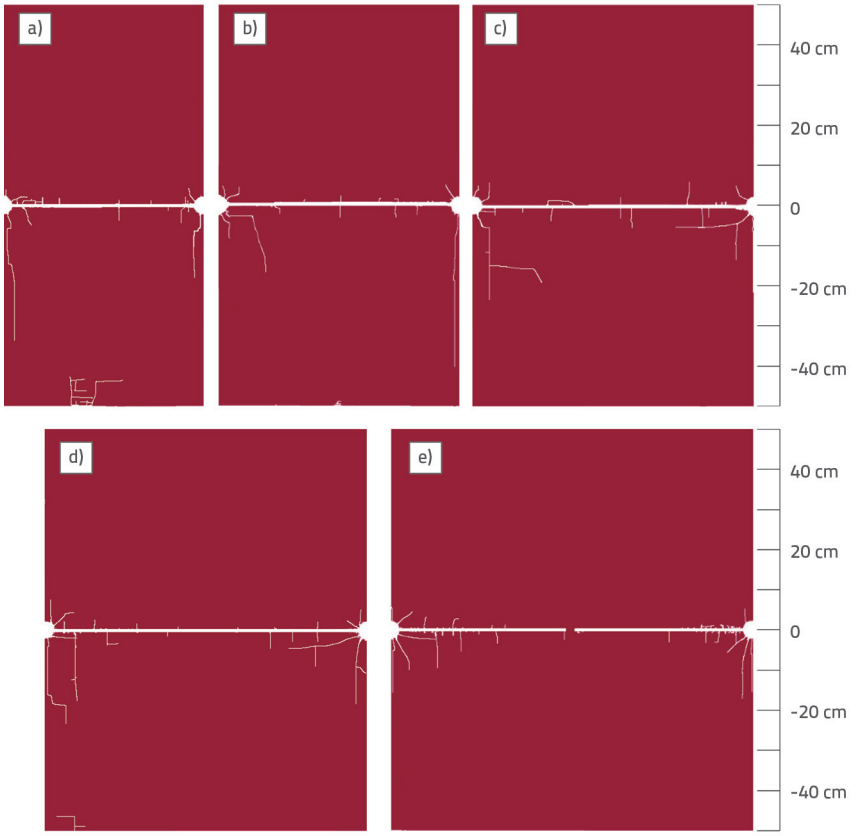

Flgure 6. Effect of controlled shaped-charge blasting under different hole spacings: a) 50 cm; b) 60 cm; c) 70 cm; d) 80 cm; e) 90 cm

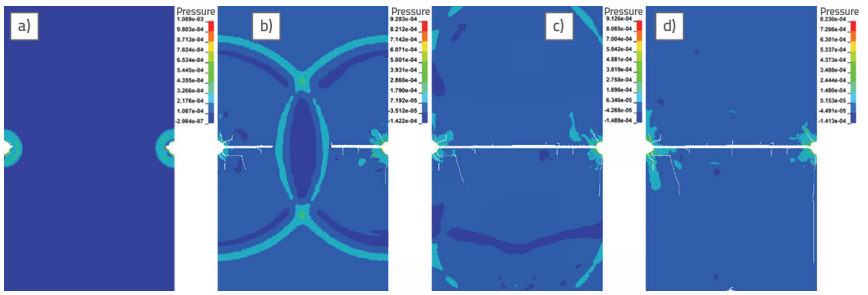

Figure 7. Crack propagation process of controlled shaped-charge blasting: a) t = 10 μs; b) t = 100 μs; c) t = 220 μs; d) t = 600 μs

In summary, controlled shaped-charge blasting can produce a clear effect on the formation of directional cracks and can still achieve crack penetration between holes when the spacing between the two holes is 80 cm. Simultaneously, controlled shaped-charge blasting can avoid the phenomena of over-excavation and under-excavation, reduce the damage to the surrounding rock, improve the stability of the excavation chamber, obtain a flat contour surface, and realise the effect of fine-controlled blasting excavation.

To reflect the entire process of initiation, propagation, and penetration of controlled shaped-charge blasting cracks more intuitively, a calculation model with spacing of 60 cm between holes was considered as an example to analyse the propagation process of explosion-induced cracks between two holes after detonation. As shown in Figure 7, 20 μs after the explosive initiation, the wall of the blast hole was subjected to a strong blast impact. Because the shaped-charge groove produced a guiding effect on the explosion energy, the rock of the wall of the blast hole was subjected to a violently shaped gas jet in the direction of the shaped charge, thereby forming initial cracks in the wall of the blast hole. Subsequently, the explosive gas rapidly wedged into the initial cracks, which caused the cracks to expand in the straight direction of the blast hole to form the main crack, and a small number of secondary cracks were formed on both sides of the main crack. At 200 μs after detonation, the main cracks of the two blast holes were connected in a direction roughly parallel to the line between the blast holes, whereas the cracks further expanded in other directions around the blast holes. After the main crack was connected, the explosive gas continued to expand within the crack, promoting an increase in the crack width. Under the action of the reflected tensile waves, the crack extended to the free surface. With the dissipation and attenuation of energy, cracks stop expanding in the rock.

A comprehensive comparative analysis of the distribution law of blast-induced cracks under these two different blasting methods shows that controlled conventional blasting methods can only form connecting cracks in the straight direction between the blast holes when the hole spacing is relatively small, and the formation effect of directional cracks is relatively poor. This is not conducive to the formation of a flat contour surface, and predominant over- and underbreaks occur in the actual blasting construction process. Many cracks are formed on the side of the retained rock mass, extending into the surrounding rock, which causes a high degree of damage to the surrounding rock and affects the safety and quality of blasting construction. With hole spacing of 50–80 cm, controlled shaped-charge blasting formed connecting cracks in the straight direction between the blast holes, and the formation effect of directional cracks was ideal. The secondary cracks that formed on both sides of the main crack and those formed in other directions of the blast hole were smaller in number and shorter in length, and the degree of damage to the surrounding rock was low. The quality of the excavation can be improved while meeting the requirements of field-blasting excavation.

4. In situ test of controlled shaped-charge blasting

4.1. Engineering overview of the field test site

The Tianchi pumped-storage power station is located in the Henan Province. It consists of an upper reservoir, water transmission system, underground powerhouse system, lower reservoir, and switching station. Four electric generating units with a single installed capacity of 300 MW were installed in the underground powerhouse, for a total installed capacity of 1200 MW. The normal storage water level of the upper reservoir is 1063.0 m, with a corresponding storage capacity of 14.05 million m³; the level of dead water is 1020.0 m, with a corresponding storage capacity of 2 million m³, and the adjusted storage capacity is 12.05 million m³. The normal storage water level of the lower reservoir is 537.5 m, with a corresponding storage capacity of 16.34 million m³; the level of dead water is 510.0 m, with a corresponding storage capacity of 4.31 million m³, and the adjusted storage capacity is 12.03 million m³. An overall diagram of the Tianchi pumped storage power station is shown in Figure 8.

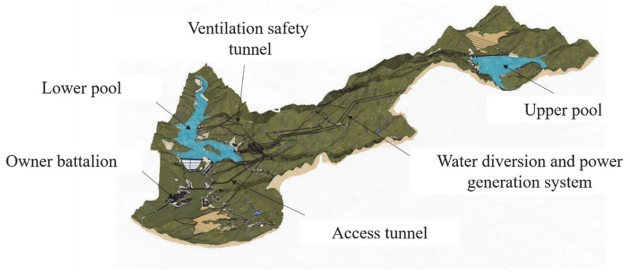

Figure 8. Overall diagram of the Henan Tianchi pumped storage power station

4.2. Construction technology with controlled shaped-charge blasting

Shaped-charge method: The explosives were filled into a PVC energy-gathering pipe. A schematic of the structure of the shaped-charge tube and a diagram of the shaped charge are shown in Figure 9.

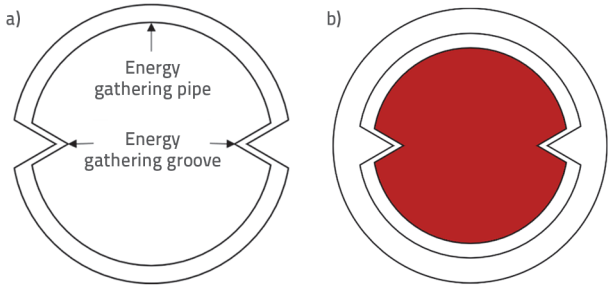

Figure 9. Schematic of the shaped-charge method: a) Shaped-charge tube structure; b) Shaped-charge situation

The material for the energy-gathering pipes was PVC, as shown in Figure 10. Additional process: The shaped-charge operation proceeds by loading the explosive into the shaped-charge tube, as shown in Figure 11.

Figure 10. Schematic of the shaped-charge tube

Figure 11. Charging operation of the shaped-charge tube

4.3. Drilling and blasting design of controlled shaped-charge blasting

According to the numerical analysis, the hole spacing in controlled conventional blasting should not exceed 50 cm, whereas controlled shaped-charge blasting can produce a directional crack effect when the spacing between two blast holes is 80 cm. Therefore, combined with the actual geological conditions of the tailwater tunnel of the Tianchi pumped storage power station, the spacing of the blast holes was increased from approximately 50 cm to 75 cm in the design scheme of controlled shaped-charge blasting, and the layout of the blast holes, auxiliary holes, and blasting parameters were consistent with the design of conventional smooth blasting. The hole layout for controlled shaped-charge blasting is shown in Figure 12, and the hole section layout is shown in Figure 13. The blank area between the parts of the explosive charge represents air, the strengthening charge represents the bottom strengthening charge, and the mass ratio of the charge to the bottom mass charge is 0.7, as shown in Figure 14. The specific drilling and blasting parameters are listed in Table 6.

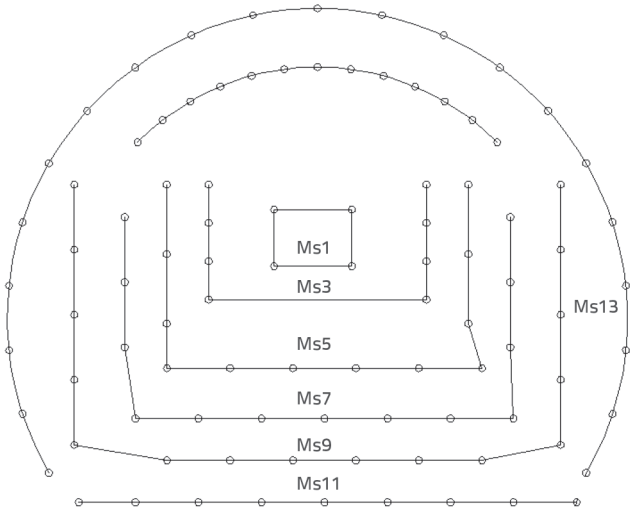

Figure 12. Schematic of hole layout in controlled shaped-charge blasting

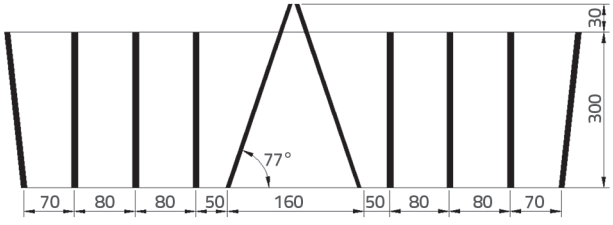

Figure 13. Schematic of section layout of blast holes (Unit: cm)

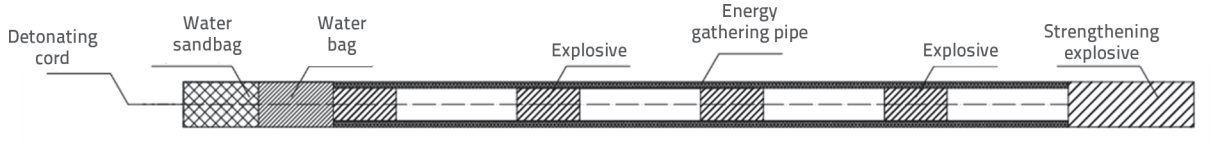

Figure 14. Schematic of the charging structure of holes in controlled shaped-charge blasting

Table 6. Design parameters of controlled shaped-charge blasting

Hole designation	Number of holes (A)	Hole depth [m]	Hole charge		Number of detonator segments (section)
			Mass per hole [kg/hole]	Total mass [kg]	
Cut slot	4	3,4	2,2	8,8	Ms1
Auxiliary hole	8	3	2	16	Ms3
Auxiliary hole	12	3	2	24	Ms5
Auxiliary hole	26	3	2	52	Ms7
Auxiliary hole	16	3	2	32	Ms9
Bottom hole	9	3	2	18	Ms11
Contour pore	21	3,1	0,6	12,6	Ms13
Total	96	/	/	163,4	/

4.4. In situ testing

4.4.1. Layout of measuring points

To obtain a quantitative index for evaluating the influence of the blasting excavation on the stability of the surrounding rock of the tunnel, an L20 blasting vibration meter produced by Chengdu Jiaobo Science and Technology Co., Ltd. was used to test the vibration velocity of the blasting excavation and monitor the vibration effect of the blasting excavation on the surrounding rock of the tunnel. The performance of the selected instrument is satisfactory; it can measure vibration waves in three different directions simultaneously. The test speed was maintained at 0.001–35.5 cm/s, the test frequency range was controlled at 1–1000 Hz, the test accuracy was 5 %, and the reading accuracy of the instrument was 0.1 %. The vibrometer and vibration sensor are shown in Figure 15.a, and the on-site instrument installation is shown in Figure 15.b.

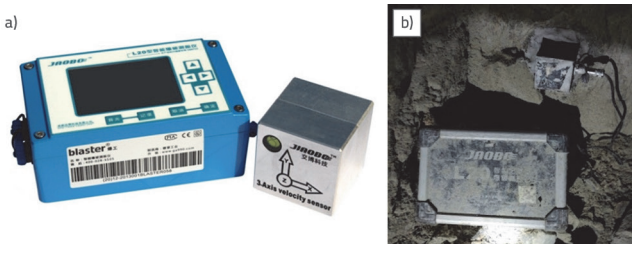

Figure 15. Instrument and installation on site: a) Blasting vibration meter; b) Installation of instrument on site

According to the requirements of blasting vibration monitoring in blasting safety regulations, the vibration effects in the middle and far regions of the blasting source are mainly investigated during testing. Therefore, to obtain the vibration velocity in the middle and far regions of the blast source after blasting, the test instruments were installed on the wall of the tunnel at a horizontal distance of 10 m from the face of the blasting excavation. The vertical height of each measuring point from the ground was approximately 0.5 m, and five measuring points were arranged along the axis of the tunnel. The measurement points are denoted as M1, M2, M3, M4, and M5, from near to far. The arrangement of the measurement points is shown in Figure 16.

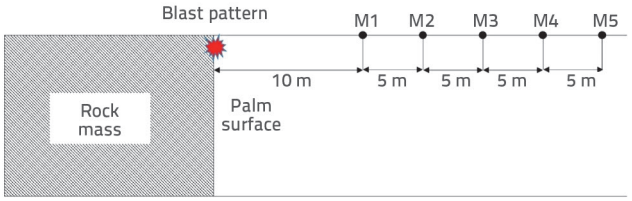

Figure 16. Layout diagram of blasting vibration measurement points

4.4.2. Material preparation and test process

The pipe used in the field test of controlled shaped-charge blasting in the tail water tunnel of Tianchi pumped storage power station was shaped like a "C", and the length of each shaped-charge tube was divided into 1, 2, 3 m, and other standard sizes. The drilling depth of the blast holes for the controlled shaped-charge blasting was 3 m. Therefore, to facilitate the operation, reduce the charging time, and improve the construction efficiency, the length of the shaped-charge tube used for charging during the test was set to 1 m, and two shaped-charge tubes were loaded into each contour blast hole. In the shaped-charge charging process, the emulsion explosive was evenly divided into two parts horizontally, loaded into the shaped-charge tube at axial intervals, and the detonating cord was connected simultaneously. The entire charging process is simple and efficient, without the need for other complicated operational procedures. The structure of the shaped charge is shown in Figure 17.

In addition, water bags (Figure 18) and water–sand bags matching the aperture of the blast holes were used to block the orifice, reduce the tedious and time-consuming process of hole stemming, and improve the efficiency of the overall charging process. The use of water bags and water–sand bags to seal the blast hole can reduce the dust caused by rock breakage after blasting, improve the air quality in the tunnel after blasting, enhance the safety of the construction environment, and improve the physical and psychological health of the

construction workers. Because of the small excavation section of the test, manual production of the required water bags and water–sand bags can meet these requirements. The ratio of water to river sand in the water–sand bags was 0.5.

Figure 17. Charging and installation of shaped-charge tube on site: a) Charging of shaped-charge tubes; b) Site installation

The produced water bags and water–sand bags should have no air bubbles inside, and the filling expansion should be sufficient to achieve the best sealing effect in the blast hole.

Figure 18. Water bags and site usage: a) Water bags and water–sand bags

Figure 18. Water bags and site usage: b) Hole plugging with water–sand bags

4.5. Analysis of experimental results

By observing and recording the half-hole marks left in the tunnel wall after the blasting excavation and the flatness of the excavation contour surface, the half-hole rate data of controlled conventional blasting and controlled shaped-charge blasting were obtained, as listed in Table 7.

It can be observed from the data in Table 7 that when controlled conventional blasting is used for excavation, the half-hole rate is only 38 %, which indicates that the excavation caused significant damage to the surrounding rocks, and obvious over- and under-excavation phenomena occurred. When controlled shaped-charge blasting was used for excavation, the half-hole rate reached 95 %, that is, the half-hole rate after blasting increased by 57 percentage points compared with that after controlled conventional blasting, indicating that the controlled shaped-charge blasting method can obtain a flat contour surface and reduce the degree of damage to the surrounding rocks. According to the geological data of the power station, the rock surrounding the blasting test site is hard rock. As indicated in Table 8, the half-hole rate of controlled conventional blasting was less than 50 %, and the excavation quality was poor.

Table 7. Statistical table of half-hole rate

Blasting method	**Number of contour holes** [number]	**Half-hole number** [number]	**Half-hole rate** [%]
Controlled conventional blasting	32	12	38
Controlled shaped-charge blasting	21	20	95

Table 8. Evaluation criteria for half-hole rate

Lithology / **Half-hole rate** [%]	**Quality grade**			
	Good	**Better**	**In general**	**Poor**
Hard rock	> 90	70 – 90	50 – 70	< 50
Middle rock	> 70	50 – 70	30 – 50	< 30
Soft rock	> 50	30 –5 0	20 – 30	< 20

Conversely, the half-hole rate of controlled shaped-charge blasting was greater than 90 %, and the excavation quality grade was good, highlighting the superiority of controlled shaped-charge blasting in actual excavations. Combined with the contour effect obtained in the field excavation, it can be observed in Figure 19 (a) that the formation quality of the tunnel wall under controlled conventional blasting was poor, and there was an obvious over-excavation phenomenon. The depth of the over-excavation was approximately 20 cm, which caused serious damage to the retained rock mass. The blasting effect was unsatisfactory and did not meet the construction requirements. Simultaneously, according to Figure 19 (b), with a reduction in the number of blast holes by 30 % and the corresponding reduction in the amount of explosives, the contour surface of the tunnel obtained after controlled shaped-charge blasting was very smooth and flat, and clearly visible half-hole marks remained on the contour surface of the tunnel after blasting. It was shown that a good directional crack-forming effect can be obtained using the controlled shaped-charge blasting method in an actual excavation, with the energy of the explosive fully acting on the rock mass in the direction of the connection between the blast holes through the guiding effect of the shaped-charge groove. This can cause the rock mass to produce directional cracks, reduce the damage in the connection direction of the blast holes, reduce the degree of damage to the surrounding rock, and improve the safety and stability of underground blasting construction. High-quality and high-efficiency blasting excavations are achieved.

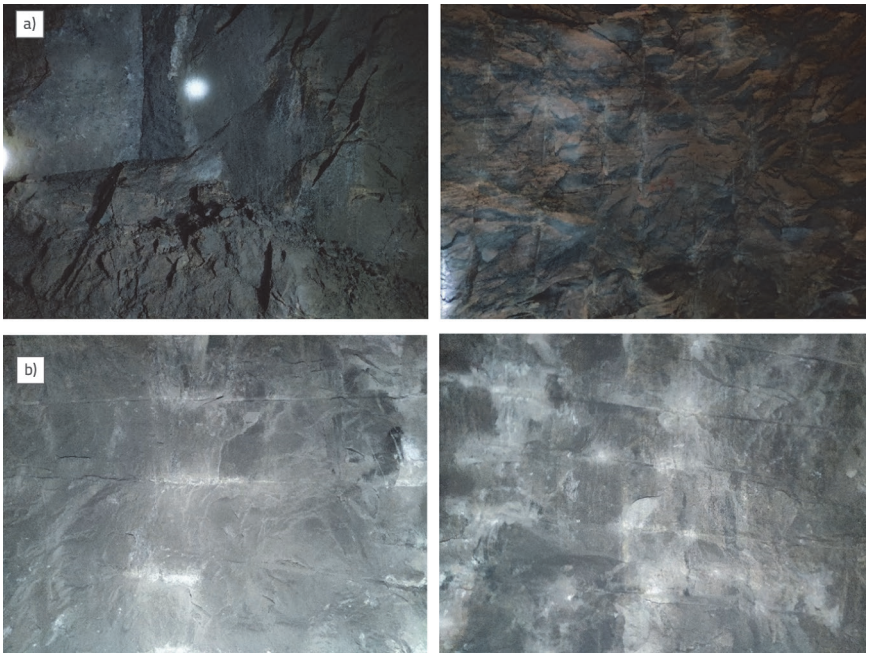

Figure 19. Excavation contour effect of controlled conventional blasting and controlled shaped-charge blasting: a) Excavation contour surface produced using controlled conventional blasting; b) Excavation contour surface produced by controlled shaped-charge blasting

4.6. Discussion on vibration monitoring results

The specified vibration velocities are the maximum values for the entire event measured in the blast vibration analysis. By monitoring the vibration velocity of controlled conventional blasting and controlled shaped-charge blasting three times, the vibration velocity components monitored by the instrument in each test were analysed in three directions, in which the longitudinal direction is parallel to the axis of the tunnel, the vertical direction is perpendicular to the horizontal plane, and the transverse direction is horizontal and perpendicular to the axis of the tunnel. The test results of conventional blasting are listed in Table 9, and the test results of controlled shaped-charge blasting are listed in Table 10. D represents the blasting centre distance, V_L denotes the vibration velocity in the longitudinal direction, V_v represents the vibration velocity in the vertical direction, and V_T designates the vibration velocity in the transverse direction. The curves of the test results are shown in Figure 20. The variation trends of the peak vibration velocity in controlled conventional blasting and controlled shaped-charge blasting were approximately similar, as shown in Figure 20. With the increase in the distance between the measuring point and detonation source, the peak vibration velocity in all directions of controlled conventional blasting and controlled shaped-charge blasting had an obvious decreasing trend. The peak vibration velocity curves of controlled shaped-charge blasting and controlled conventional blasting show that the peak vibration velocity attenuated faster when the distance from the detonation source was closer to the measuring point, whereas the peak vibration velocity attenuated slowly when the distance from the detonation source was farther, which was more prominent in controlled shaped-charge blasting. The typical phenomena and laws were observed by comparing the vibration monitoring results of the three groups. In the first set of tests, the maximum vibration velocity of controlled conventional blasting was the longitudinal vibration velocity, which reached 5.68 cm/s. The maximum vibration velocity of the controlled shaped-charge blasting was 4.60 cm/s in the longitudinal direction. In the second set of tests, the maximum vibration velocity of the controlled conventional blasting was 6.28 cm/s in the longitudinal direction and that of the controlled shaped-charge blasting was 5.23 cm/s, also in the longitudinal direction. In the third set of tests, the maximum vibration velocity of the controlled conventional blasting was 6.32 cm/s in the longitudinal direction

Table 9. Summary of test results of conventional blasting

Test number	Measure point number	D [m]	V_L [cm/s]	Dominant frequency, f [Hz]	V_V [cm/s]	Dominant frequency, f [Hz]	V_T [cm/s]	Dominant frequency, f [Hz]
1	MP1	10	5.68	109.9	3.91	359.9	4.03	420.9
	MP2	15	3.35	203.8	3.12	203.8	3.28	123.8
	MP3	20	2.60	57.2	2.16	57.2	1.81	312.2
	MP4	25	1.48	274.7	2.09	169.2	1.48	95.7
	MP5	30	1.01	123.8	1.75	137.9	1.03	95.8
2	MP1	10	6.28	156.2	4.47	91.9	5.47	156.2
	MP2	15	3.82	142.2	3.23	142.2	2.99	30.2
	MP3	20	3.29	403.6	3.42	127.4	2.90	29.2
	MP4	25	1.50	95.1	2.35	95.4	1.49	142.9
	MP5	30	1.24	113.2	1.97	83.4	1.23	285.2
3	MP1	10	6.32	313	4.48	90.1	5.98	260.4
	MP2	15	2.98	176	3.93	85.2	2.98	293
	MP3	20	2.52	313	2.91	88.4	2.48	334.8
	MP4	25	1.37	156	2.15	156.2	1.76	187.5
	MP5	30	1.21	99.7	1.55	58.6	1.47	195.3

Table 10. Summary of test results of controlled shaped-charge blasting

Test number	Measure point number	D [m]	V_L [cm/s]	Dominant frequency, f [Hz]	V_V [cm/s]	Dominant frequency, f [Hz]	V_T [cm/s]	Dominant frequency, f [Hz]
1	MP1	10	4.60	31.9	3.07	156.2	4.10	312.5
	MP2	15	2.56	59.2	2.35	3.5	2.57	142.2
	MP3	20	2.38	137.9	2.21	59.2	1.54	142.9
	MP4	25	1.23	33.5	1.69	132.5	1.22	8.5
	MP5	30	0.90	102.7	1.47	97.4	0.91	7.9
2	MP1	10	5.23	234.1	3.35	99.7	4.54	76.8
	MP2	15	2.91	162.2	2.58	104.2	2.78	97.7
	MP3	20	2.80	123	2.35	260.4	1.82	293
	MP4	25	1.28	82.2	1.81	66	1.27	79.4
	MP5	30	1.02	85.2	1.61	73.2	1.01	82.2
3	MP1	10	4.56	173.6	3.24	66	5.21	15.7
	MP2	15	2.46	93.8	3.39	156.2	2.46	82.2
	MP3	20	2.42	93.8	2.36	75.6	1.98	85.2
	MP4	25	1.21	114.3	1.76	63.3	1.48	82.2
	MP5	30	0.87	76.8	1.47	80.8	1.34	76.8

and that of the controlled shaped-charge blasting was 5.21 cm/s in the transverse direction.

The results of the three blasting vibration monitoring tests show that the peak vibration velocity produced by controlled conventional blasting and controlled shaped-charge blasting is within the safety standard range for tunnel blasting excavation. The safety standard range for tunnel blast excavation is such that the peak vibration velocity of the measuring point at a horizontal distance of 10 m from the explosion source should be less than 10 cm/s. The peak vibration velocity of each measuring point of the three groups in all directions of the controlled conventional blasting was greater than that of the corresponding measuring point of the controlled shaped-charge blasting, and the peak vibration velocity of the controlled shaped-charge blasting was reduced by 10 % to 21 % compared with that of the controlled conventional blasting. This indicates

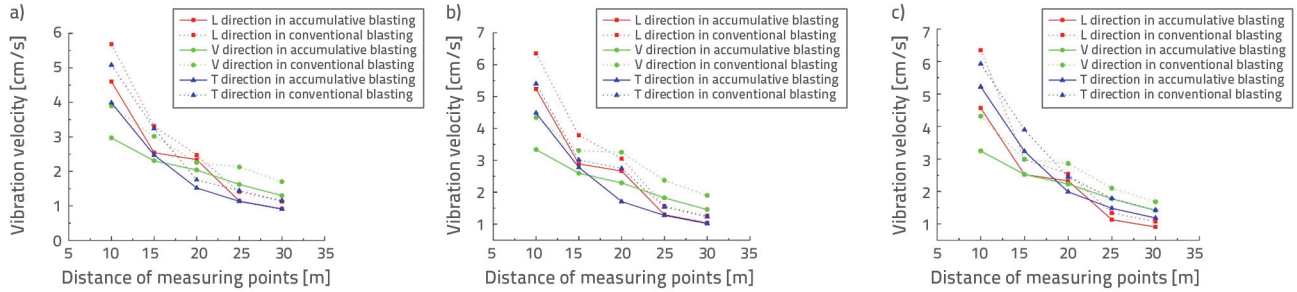

Figure 20. Comparison of peak vibration velocity in three blasting tests: a) First test; b) Second test; c) Third test

that the controlled shaped-charge blasting can apply more explosive energy to the formation of directional cracks between the two holes and the broken rock. This can effectively reduce the blasting vibration velocity and cause less damage to the reserved rock mass, which is conducive to the stability of the underground chamber and guarantees construction quality more effectively.

5. Conclusion

In this study, the actual engineering problems encountered in the blasting excavation of the underground tunnel of the Tianchi pumped storage power station in China were considered as the research background. The ANSYS/LS-DYNA dynamic finite element software was used to perform numerical calculations and analyses, and the stress characteristics of the tunnel under the condition of in situ stress were analysed. A two-dimensional fluid–solid coupling model was established to simulate rock blasting, and the crack propagation effects between the blast holes under controlled conventional blasting and controlled shaped-charge blasting were compared and analysed. The directional crack formation mechanism of controlled blasting and the distribution law of cracks under different hole spacings and in situ stresses were examined, and the numerical analysis results were verified by an in situ test. The main conclusions are as follows.

- Combined with the smooth blasting excavation method, the dynamic finite element software ANSYS/LS-DYNA was used to analyse the stress characteristics of the three-dimensional tunnel blasting excavation model, and the stress distribution state of the blasting layer under initial stress conditions was obtained.
- When the diameter of the blast hole is 42 mm, controlled conventional blasting can form cracks approximately along the connection direction between the blast holes with hole spacing of 50 cm, which is approximately 12 times the diameter. The damage depth of the surrounding rock is up to 40 cm, which is not conducive for obtaining a flat contour surface after blasting. Controlled shaped-charge blasting can form cracks approximately along the connection direction between the blast holes with hole spacing of 80 cm, which is approximately 20 times the diameter. The damage depth of the surrounding rock is controlled to within 15 cm, which is conducive to obtaining a complete contour surface after blasting.
- The field blasting test results show that the blast hole spacing of controlled shaped-charge blasting increases by 50 % compared with that of controlled conventional blasting, and the half-hole rate increases by 57 percentage points after excavation. The vibration monitoring results of in situ blasting show that the peak vibration velocity caused by controlled shaped-charge blasting is reduced by 10 %–21 % compared to that of controlled conventional blasting. In the blasting excavation of a deep tunnel, a smooth and flat contour surface is obtained using controlled shaped-charge blasting, and an ideal directionally controlled blasting effect is achieved.

Acknowledgments

This study was supported by the Doctoral Scientific Research Foundation of Shandong Technology and Business University, China (Grant No. BS202009), the National Natural Science Foundation of China (Projects No. 51804178 and No. 52109165), and the Doctoral Scientific Research Foundation of Shandong Technology and Business University, China (Grant No. BS201931).

REFERENCES

[1] Wei, W.L., Chen, Y.Q., Ren, X.J., Wang, J.H., Wang, Z.Q., et al.: Experimental and numerical study on the influence of plastic modified concrete as attenuation layer on explosion effect. International Journal of Structural Stability and Dynamics, 2250116 (2022), https://doi.org/10.1142/S0219455422501164.

[2] Pugh, E.: Theory of Jet Formation by Charges with Lined Conical Cavities, 1952.

[3] Hirsch, E.: The natural spread and tumbling of the shaped charge jet segments. Propellants, Explosives, Pyrotechnics, 6 (1981) 4, pp. 104-111.

[4] Hayes, G.: Linear shaped-charge (LSC) collapse model. Journal of materials science, 19 (1984) 9, pp. 3049-3058.

[5] He, M., Cao, W., Shan, R., et al.: New technique of bidirectional shaped charge tensile blasting. Chinese Journal of Rock Mechanics and Engineering, 12 (2003), pp. 2047-2051.

[6] Fu, L., Wang, W., et al.: Comparison of jet forming mechanism between ring and linear shaped charge. Journal of Naval Aeronautical and Astronautical University, 29 (2014) 5, pp.470-474.

[7] Duan, B., Zhou, Y., Zheng, S., et al.: Blasting demolition of steel structure using linear cumulative cutting technology. Advances in Mechanical Engineering, 9 (2017) 11, 2071941996.

[8] Xu, W., Wang, C., Chen, D.: The jet formation and penetration capability of hypervelocity shaped charges. International Journal of Impact Engineering, 132 (2019).

[9] Wang, F., Li, B., et al.: Effect of cone angle on cutting performance of linear shaped charge. Initiators and pyrotechnics, 3 (2019), pp. 22-25.

[10] Wan, D., Zhu, Z., Liu, R., Liu, B., Li, J.: Measuring method of dynamic fracture toughness of mode I crack under blasting using a rectangle specimen with a crack and edge notches. International Journal of Rock Mechanics and Mining Sciences, 123 (2019),104104, https://doi.org/10.1016/j.ijrmms.2019.104104.

[11] Li, H., Liu, T., Liu, Y., Li, J., Xia, X., Liu, B.: Numerical modeling of wave transmission across rock masses with nonlinear joints. Rock Mechanics and Rock Engineering, 49 (2019) 3, pp. 1-7, https://doi.org/10.1007/s00603-015-0766-2.

[12] Li, B.: Numerical Simulation of Elastic Resistance of Gradient Composites. Changsha: Central South University, 2013.

[13] Liu, H., Lv, S., Zhang, L., Yuan, X.: A dynamic damage constitutive model for a rock mass with persistent joints. International Journal of Rock Mechanics and Mining Sciences, 75 (2015), pp. 132-139, https://doi.org/10.1016/j.ijrmms.2015.01.013.

[14] Huang, J., Li, X., Luo, Y., Liu, T., Dong, Q., Xu, K.: Numerical simulation of influence of filled joint on the crack formed by notch hole blast. European Journal of Environmental and Civil Engineering, 2017 (2017), pp. 1-17, https://doi.org/10.1080/19648189.2017.1392366.

[15] Wang, Z., Li, Y., Shen, R.: Numerical simulation of tensile damage and blast crater in brittle rock due to underground explosion [J]. International Journal of Rock Mechanics and Mining Sciences, 44 (2007) 5, pp. 730-738.

[16] Xie, H., Ruan, H.: Directional fracture blasting numerical simulation and experimental study, Chengdu, China: IEEE Computer Society, 2012.

[17] Yang, R., Bawden, W.F., Katsabanis, P.D.: A new constitutive model for blast damage. International Journal of Rock Mechanics and Mining Sciences and Geomechanics Abstracts, 33 (1996) 3, pp. 245-254, https://doi.org/10.1016/0148-9062(95)00064-X.

[18] Xiao D., Li B., Pu C., et al.: Model test and numerical simulation for directional pressure relief blasting, Taichung, Taiwan: Trans Tech Publications Ltd., 2013.

[19] LS-DYNA keyword user's manual Version 971, Livermore Software Technology Corporation (LSTC), 2007.

[20] Zhou, Y., Gou, D., et al.: Numerical simulation analysis of rock breaking effect of cumulative blasting. Safety in coal mines, 45 (2014) 12, pp. 218-220.